

Thermal Transients During Processing of 3003 Al-H18 Multilayer Build by Very High-Power Ultrasonic Additive Manufacturing

M.R. SRIRAMAN, MATT GONSER, DANIEL FOSTER, HIROMICHI T. FUJII, S.S. BABU, and MATT BLOSS

Previous investigations suggested a gradient in bond microstructure along the height of a “build” made by very high power ultrasonic additive manufacturing—a rapid prototyping process that is based on ultrasonic seam welding. The bonding of foils is associated with the occurrence of dynamic recrystallization at the interfaces between them. To understand heating patterns across the build that may be responsible for such microstructure evolution, temperatures from different interface regions were recorded simultaneously during the fabrication of a 3003 Al-H18 multilayer build under a given processing condition. Thermal transients were observed over multiple interfaces of the build during welding of each layer. The temperatures were the highest for the layer processed and were found to diminish beneath with each subsequent layer. Such maximum temperatures also depended on the height at which the new layer was bonded. The occurrence of transients across the build is rationalized based on heat being conducted away from the processed layer.

DOI: 10.1007/s11663-011-9590-6

© The Minerals, Metals & Materials Society and ASM International 2011

I. INTRODUCTION

ULTRASONIC additive manufacturing (UAM) is a rapid prototyping process that uses metallic foils/tapes (typically 100 to 150 μm thick and 25 mm wide) for the fabrication of three-dimensional (3-D) solid parts of near-net shape.^[1] The process that works on the principle of ultrasonic seam welding involves the application of lateral ultrasonic vibrations (typically 20 kHz) to the metal tape through a sonotrode. The governing parameters are vibration amplitude, static normal force, travel speed, and preheat temperature. The sonotrode surface texture (described subsequently) has a significant effect on the process as well. The tape making contact with the sonotrode at any instant is subject to vibrations at the chosen amplitude relative to the substrate under a normal force as the sonotrode rolls along its length at the chosen travel speed. Bonding of the faying surfaces, in the solid state, is facilitated by the rapid disruption of oxide layers on either surfaces and the establishment of nascent metal–metal contact.^[1,2] Typically, the first tape is welded on to a base plate. For the sonotrode to subject the tape to vibrations, a surface texture is

imparted to it, which allows it to embed into the tape that it makes contact with, at any given instant. As the sonotrode moves to its next position, it disengages itself from this region and embeds into the next, and so forth. This alternate engaging and disengaging action leaves behind a rough imprint over the foil surface along its length. As the next tape is welded on to such a surface, it could potentially leave some unbonded regions or voids. This process is repeated layer after layer until a “build” or part of required dimensions is produced. Intermediate machining operations are performed usually during this “additive” process, depending on the features required to be incorporated into the part as it is being built.^[1] Components of intricate shapes/details and parts with embedded sensors/electronics are possible with this method.^[3] Limitations with the currently available commercial UAM machines (hereinafter referred to as low-power UAM machines or simply UAM machines) in terms of amplitude/force levels^[3–5] have led to the development of the very high power ultrasonic additive manufacturing (VHP UAM) machine.^[3] Rated at 9 kW (three times more than low-power UAM machines), this equipment employs two transducers operating in tandem to provide increased vibration amplitudes of up to 52 μm to the sonotrode (as opposed to 30 μm in UAM machines) under force levels of up to 15 kN (seven times larger than UAM machines).^[3,6,7] A schematic of the system is shown in Figure 1. Similar metal welding of different Al alloys, copper, and stainless steel without any external heating has been possible using this machine.^[6–10]

Bonding between tapes in VHP UAM is observed to occur through dynamic recrystallization (DRX) at the interfaces.^[6–9,11] Our previous investigations^[7,11] showed

M.R. SRIRAMAN, Researcher, DANIEL FOSTER, Graduate Student, and S.S. BABU, Associate Professor, are with the Department of Materials Science and Engineering, The Ohio State University, Columbus, OH 43221. Contact e-mail: babu.13@osu.edu MATT GONSER, Postdoctoral Fellow, is with the College of Engineering & Engineering Technology, Northern Illinois University, De Kalb, IL 60115. HIROMICHI T. FUJII, Assistant Professor, is with Tohoku University, Aoba-ku, Sendai 980-8576, Japan. MATT BLOSS, Technology Leader, is with the Edison Welding Institute, Columbus, OH 43221.

Manuscript submitted April 1, 2011.

Article published online October 27, 2011.

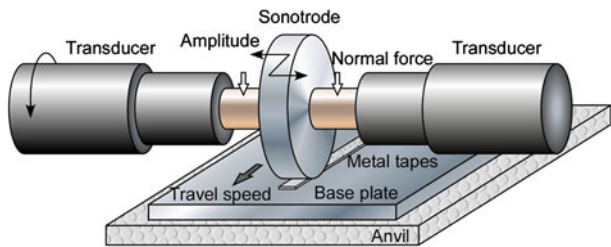


Fig. 1—chematic showing the double transducer-sonotrode assembly used in the VHP UAM process.

that heating, so as to cause DRX, is related to dynamic plastic shearing of contacting asperities under high strains. With very high strain rates being involved as well,^[5,6,12,13] the heating is hypothesized to take place under adiabatic conditions,^[14,15] causing a sharp temperature rise promoting DRX. Such heating at the weld regions is also transient in nature.^[11] Processing of every layer in a multilayer build would therefore be associated with the occurrence of thermal transients that could influence the microstructure and properties of the build. Our past research^[9] on 3003 Al-H18 “step build” processed by VHP UAM comprising of 2, 4, 6, and 8 layers along different regions of the seam (Figure 2^[9]) suggests an increased effect of temperature on the resulting microstructure toward the bottom layers/interfaces (Figure 3^[9]). The second interface (from the bottom) in an eight-layer-tall build for instance, was found to have a greater span in terms of the dynamically recrystallized grain structure than the corresponding interface in a two-layer build (Figure 3^[9]). Evidence of recrystallization was also found away from such interfacial regions with the taller build (Figure 3^[9]). This could manifest itself in terms of a gradient in the bonding quality of the layers, with possible improved bonding of bottom layers compared with the top. Although the observation made^[9] was attributed to a “cumulative” effect, it is not clear whether this is simply a result of multiple thermal cycles experienced by the bottom layers because of heat conducted from above (everytime a new layer is bonded) or whether it is because of any other mechanism. Previous studies on low-power UAM of 3003 Al-H18,^[16] carried out as part of our overall research activities, suggested the occurrence of peculiar heating (and cooling) phenomena. The observations led the investigators^[16] to postulate that the bottom layers were heating locally by friction/deformation every time a new layer was processed probably because of the general poor bond quality.^[5] Therefore, an understanding of the thermal behavior during VHP UAM was sought.

In this article, thermal transients generated during processing of a 3003 Al multilayer build by VHP UAM are investigated. The alloy typically contains (by wt pct) 1.2 Mn and 0.12 Cu, and it finds applications in the cold worked condition.^[17] Tapes from this material in the H18 (75 pct cold rolled after full annealing) condition were bonded on 3003 Al-H14 (35 pct cold rolled after full annealing) base plate for one parametric combination. The tapes were procured from United Aluminum Corporation (North Haven, CT), and the base plate was

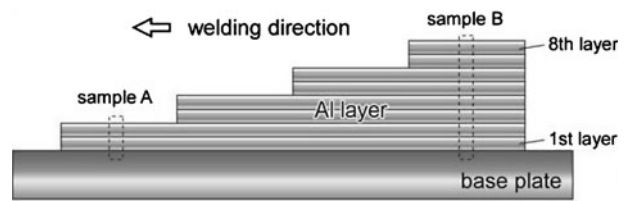


Fig. 2—Schematic of the 3003 Al-H18 step-build fabricated by VHP UAM showing the transverse sectioned samples that were characterized.^[9]

obtained from All Metal Sales Inc. (Cleveland, OH). The objectives of the investigation were to record these transients during processing of every new layer using Type K thermocouples positioned at different locations in the build and to analyze the heating/cooling patterns. Although temperature measurements have been done in the past^[12,16,18] on 3003 Al processed by low-power UAM, the investigations proposed in this study were not attempted previously. The only similar study, as mentioned, was carried out by our own group with low-power UAM (again on 3003 Al-H18).^[16] Because thermocouples are embedded easily between layers and would allow simultaneous temperature measurements from the build interior, they have been used in this investigation. However it was recognized that thermocouples would not capture the actual magnitude of the temperatures generated in a highly localized manner with a possible time resolution of $5e-5$ (1/20 kHz) seconds. This came to light during our previous set of thermal measurement studies^[11] in different alloys/processing conditions. The goal of this research therefore, was only to make comparisons between temperatures and thermal cycles generated within the build during its fabrication. Such measurements and analyses of thermal cycles (based on heat diffusion characteristics) were expected to also indicate whether parts close to solid 3003 Al (in terms of thermal behavior) could be made by VHP UAM.

II. EXPERIMENTAL PROCEDURE

A. Processing of Multilayer Build

A multilayer build of 3003 Al-H18 comprising 46 layers and 10 embedded Type K thermocouples at different locations was proposed as shown in Figure 4. Tapes of 150 μm thickness and 25.4 mm width were chosen for this purpose. The processing parameters considered were 26 μm amplitude, 5.6 kN normal force, and 35.5 mm/s travel speed. Such a processing condition, based on previous investigations,^[18,19] was found to produce good bonding between layers, both in terms of the voids left behind (void fraction of 0.02^[8]) and qualitative peel strength.^[19] A sonotrode texture of $R_a = 7 \mu\text{m}$ was chosen and no external heating was provided. The first layer was bonded to a $356 \times 356 \text{ mm}^2$ base plate measuring 12.7 mm thick. Four more layers were laid over it, which constituted the “base layers” over which the first set of three thermocouples, designated as TC1, TC2, and TC3, was placed. Although TC2 was positioned at nearly the center of the seam (75 mm), TC1 and TC3 were placed

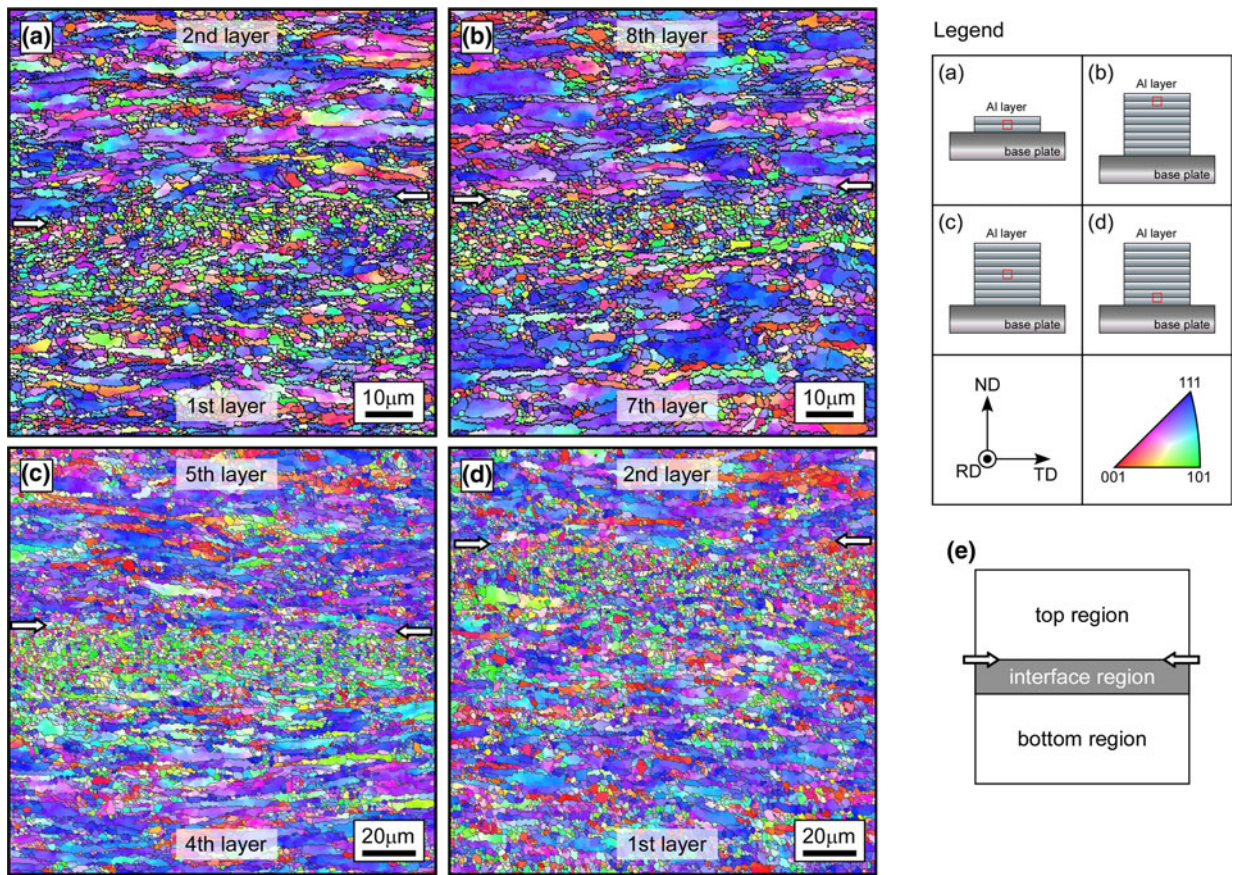


Fig. 3—Inverse pole figures from 3003 Al-H18 step build across the second interface in the 2-layer region (a), and across the eighth (b), fifth (c), and second interfaces (d), respectively, in the 8-layer region.^[9]

approximately 12.5 mm away on either side (Figure 4). They were laid flush with the tape surface, centered along the width of the tape (Section II-B) and secured firmly to the base plate by means of adhesive tapes. To ensure that the thermocouple placements were nearly horizontal and parallel to the tape surface, the height at which they were secured was adjusted correspondingly. All of them were then embedded during welding of the next tape. Figure 5 provides an illustration of how a thermocouple was typically placed on the tape surface and embedded. An additional 11 layers were bonded on to this layer before the next set of three thermocouples (TC4, TC5, and TC6) was introduced (Figure 4) and embedded as before. After the welding of another 12 layers, the third set of three thermocouples (TC7, TC8, and TC9) was embedded similarly. Finally, the one single thermocouple (TC 10) was placed on the 41st layer (after subsequent welding of 12 layers) at the center of the seam (Figure 4) and an additional 5 layers were put down to complete the 46-layer build.

B. Thermal Measurements

Type K thermocouples were chosen for this study, as mentioned previously. Each thermocouple was composed of individually sheathed, single-strand wires (Figure 5) of 42 AWG (bare wire measuring 70 μm diameter). Such thin wires were chosen for the obvious reason that they would

embed between layers easily in addition to having faster time response characteristics (compared with thicker gages). The thermocouples were prepared by unsheathing the wires to about 12 mm length, twisting them over a length of approximately 10 mm, and spot welding them at multiple locations over that length (Figure 5). This process was done to ensure that the temperature would be picked up only from the twisted and spot-welded portion (of approximately 10 mm length) of the wires (and not through any electrical short circuiting outside of this region). After testing for their electrical continuity, they were then placed at the desired locations on the tapes (as described in Section II-A) and connected to the thermal data acquisition device that had an accuracy of ± 1 K (± 1 °C).^[20] The data were collected from “start” of the seam weld to “finish,” for all layers, beginning from the sixth layer and until the last, at a sampling rate of 10,000 per second. Although the welding process was controlled through a computer, the thermal measurements had to be recorded only manually. Consequently, they were not time synchronized. However, this becomes unimportant when data comparisons between different thermocouples are made during welding of any given layer.

C. Analysis of Thermal Profiles

The temperature data acquired during processing of all layers were plotted into thermal profiles and analyzed

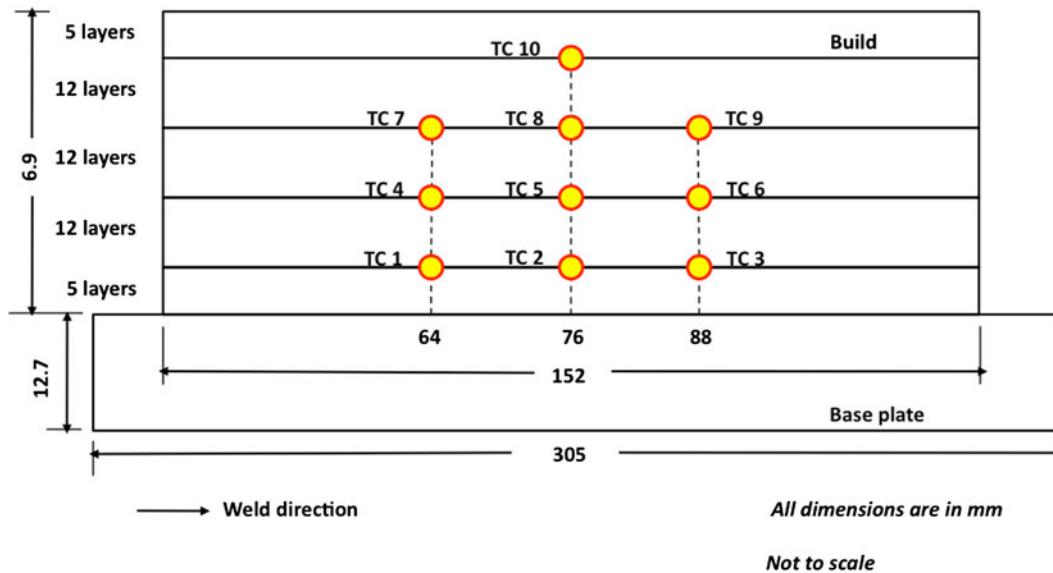


Fig. 4—Schematic of a longitudinal section of the 3003 Al-H18 multilayer build on a 3003 Al-H14 base plate with intended positions of embedded thermocouples in the build.

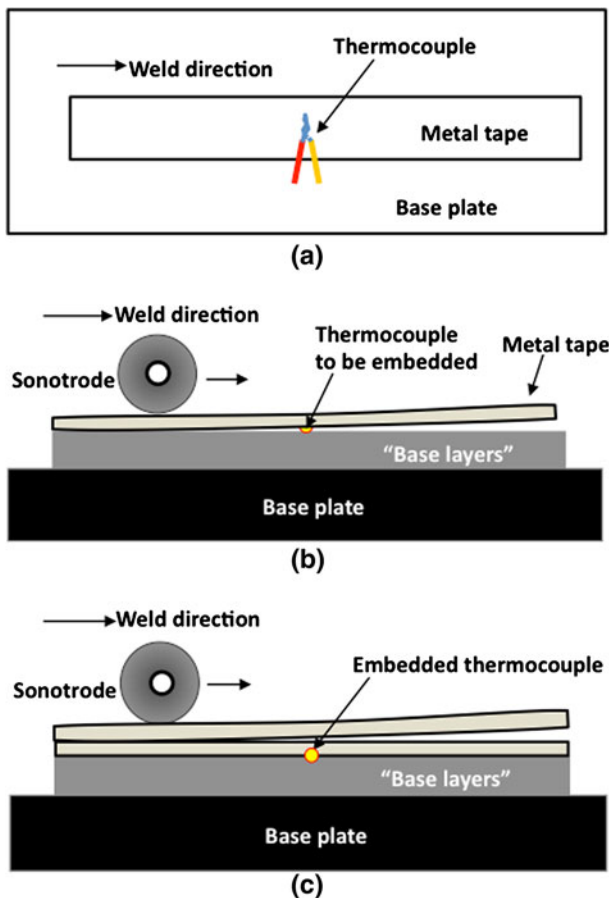


Fig. 5—Schematic showing the plan view of how the thermocouple was placed on the tape surface for embedding (a). (b) and (c) Illustrations, respectively, of the embedding of thermocouple and the welding of the next layer above.

using the commercial data processing software IgorPro (WaveMetrics, Lake Oswego, OR). The peak temperatures from the profiles were obtained typically by

interpolating and smoothing them to eliminate the noise in the data. (Much of the high-frequency noise was eliminated already during data collection because of the low-pass filtering done by the signal conditioner of the acquisition device.) Such smoothed peak temperatures were usually within ± 1 pct of the acquired peak data. In addition to comparing peak temperatures from all thermocouples and the associated time durations, the time taken for the transients in these thermocouples to register a 10 pct increase* in temperature (from room

*Although various analyses up to 50 pct increase were performed, the complete and consistent data for all thermocouples could only be achieved for 10 pct increase because of the differences in absolute peak temperatures.

temperature) was also determined. The latter analysis was chosen to observe how “stacked” thermocouples heat up during processing and to determine whether there was any localized heating that was hypothesized to occur with low-power UAM.^[16] Furthermore, the maximum heating and cooling rates in each transient were also analyzed based on the steepest portions of the heating/cooling range.

III. MODELING OF TRANSIENTS AND TEMPERATURE PREDICTIONS

To understand the heating patterns in a multilayer build, simulations of the heat front and the experimental transients were attempted. A two-dimensional (2-D) finite-element model based on COMSOL 3.5 conductive heat transfer module was employed for this purpose. The approach was to consider a moving “line” heat source (without vibrations) of “appropriate” heat flux density Q so as to simulate the heating occurring during processing of a top layer. The dimension of the heat

Table I. Conditions and Parameters Considered for 2-D Heat Conduction Finite-Element Modeling

“Build” dimensions	101.6 mm × 4.5 mm
Base plate dimensions	152.4 mm × 12.7 mm
“Coordinates” of thermocouples (TC4 and TC10 were not considered for modeling)	TC1: 38.6 mm, 0.8 mm TC2: 50.8 mm, 0.8 mm TC3: 62.2 mm, 0.8 mm TC5: 51.3 mm, 2.5 mm TC6: 62.5 mm, 2.5 mm TC7: 40.4 mm, 4.3 mm TC8: 50.3 mm, 4.3 mm TC9: 63.5 mm, 4.3 mm
Q of “line” heat source	5.1 W/mm ²
Width of heat source	2 mm
“Y position” of heat source	4.5 mm
Travel speed of heat source	35.5 mm/s
Initial temperature	297 K (24 °C)
Convection coefficient	200 × 10 ⁶ W/m ² K
Thermal conductivity of 3003 Al ^[23]	155 W/m K
Density of 3003 Al ^[23]	2730 kg/m ³
Specific heat capacity of 3003 Al ^[23]	893 J/kg K
Volumetric heat capacity of 3003 Al ^[23]	2437.89 kJ/m ³ K
Thermal diffusivity of 3003 Al ^[23]	63.58 mm ² /s

source was meant to correspond with the width of the contact between the faying surfaces. This was taken to be 2 mm based on the measurements^[10] of the width of the imprint the sonotrode left on the foil surface for an applied normal force of 5.6 kN under static conditions (without vibrations). An area of 101.6 mm × 4.5 mm corresponding to a longitudinal section of the build [comprising 30 layers and “containing” the thermocouples (Section IV-C)] positioned above the base plate of dimensions 152.4 mm × 12.7 mm was considered for modeling. A constant Q value of 5.1 W/mm², which simulated the peak temperature of a top thermocouple TC8 corresponding to processing of the 31st layer of the build (Section IV-D), was applied to the heat source to make predictions for other thermocouple locations. Although heat conduction is expected to be influenced by the presence of any defects^[21,22] between layers affecting thermal diffusivity, the use of 3003 Al thermal properties (thermal conductivity of 155 W/m K^[23]) was thought to be a good approximation. This is because, for the processing parameters employed, an average void fraction of no more than 0.02 is expected along the interfaces.^[8] The initial temperature of the build (and base plate) was taken to be 297 K (24 °C). The modeling conditions and parameters are summarized in Table I.

IV. RESULTS AND DISCUSSION

A. Thermal Transients and Interfacial Peak Temperatures

Examples of transients measured from thermocouples along a given interface are shown in Figure 6. The temperatures are observed to increase in succession from

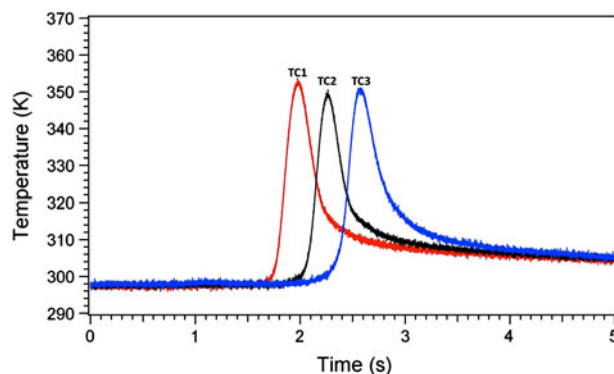


Fig. 6—Examples of thermal transients from thermocouples embedded along an interface.

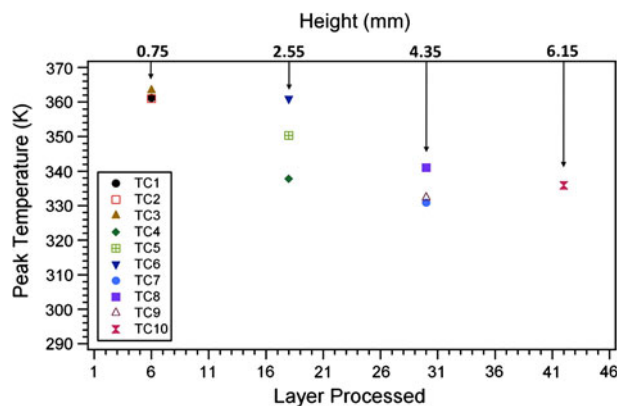


Fig. 7—Plot of peak temperatures attained for the layer processed (corresponding to embedding of thermocouples) showing a decrease in temperature with increasing layers/build height.

room temperature and attain peak values. Such peak temperatures registered from any thermocouple are expected to occur when the sonotrode is right above the location of that thermocouple. The maximum heating rates associated with these transients are found to be in the range of 530 K/s to 630 K/s (257 °C/s to 357 °C/s), whereas their cooling rates are up to 440 K/s to 510 K/s (167 °C/s to 237 °C/s). The magnitudes of these measured interfacial peak temperatures (based on their homologous values), however, may not correlate with the actual temperatures that could be generated so as to cause DRX during bonding.^[11] As mentioned in Section I, the temperatures picked up by the thermocouples could be an integrated value averaged to a resolution of 0.1 ms from a “larger” surface area of material (corresponding to the thermocouple wire diameter).

A plot of the measured peak temperatures during processing of different layers (and embedding of related thermocouples) up the build is shown in Figure 7. The maximum peak temperature recorded is approximately 363 K (90 °C) during processing of the sixth layer. It is noted that the temperatures decrease progressively from the sixth interface to the 31st interface. The extent of this drop, however, seems to diminish beyond the 31st

interface, although it would be hard to conclude so, as the value for the 42nd interface is just a single data point. A scatter in the data (sometimes up to 35 pct) as picked up by different thermocouples over a given interface was also noted (Figure 7). Such scatter could be an effect of “local” variations in contact stress/pressure under the sonotrode at any instant. This could also depend on how the twisted thermocouples sense the temperatures even as they are embedded. Higher peak temperatures were also generally found to be associated with higher maximum heating and cooling rates. These temperatures are attributed to an increased thermal energy input into the material during processing. Once a maximum temperature is attained, the cooling rate is essentially dictated by the temperature differential relative to the ambient temperature.

This result of a decreased temperature with build height may at the first instance seem to be an artifact. It is possible that in the processing of a top layer, more heat is lost into the “cold” material below than in the previous case (processing of the now bottom layer) resulting in lower measured temperatures, which are integrated average values over a large area. However, given that the heat extraction phenomenon with increasing build heights could narrow down to being 2-D in nature rather than 3-D during processing of the (now) bottom layer, such a phenomenon is unlikely.

Therefore, it seems that the actual temperature increase, attained during processing, does decrease with every new layer being added, which could result from a corresponding decrease in interfacial heating itself. What this finding probably indicates is that a loss in ultrasonic energy is transferred to the weld region. It is known from ultrasonic spot welding^[24] that a fraction of the energy applied always gets expended beneath the weld region depending on the vibration amplitude-normal force combination employed. Such an effect could manifest itself here as well. It is hypothesized that the energy transfer is influenced by a possible change in contact stress distribution in the build with the addition of every new layer. This in turn could affect processing of that particular layer. The decrease in temperatures with build height could have a bearing on the degree of bonding between corresponding layers (assuming a one-to-one relationship between bonding and temperature increase as was suggested in a previous work).^[11] However, given that the decrease in temperature, even if it were to occur, amounts to just 5 pct in terms of the homologous value (at least for this build height), it could mean only a slight decrease in bonding quality.

B. Interfacial Heating Patterns Across Build and Heating/Cooling History

With heating occurring during the welding of every layer in a multilayer build, it is evident that every interface (and bulk) beneath it experiences thermal transients. This is illustrated for the last (46th) layer processed (Figure 8). The raw data have been smoothed for better clarity. Such a temperature increase at the bottom interfaces, however, is less than what those interfaces underwent during their processing. This can

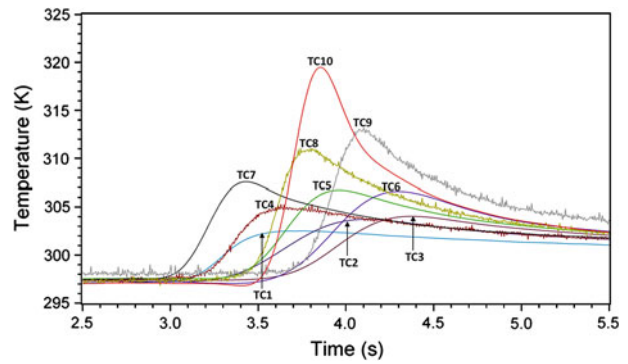


Fig. 8—Illustration of transients (smoothed) set up over the build during processing of every layer (corresponding to welding of the 46th layer).

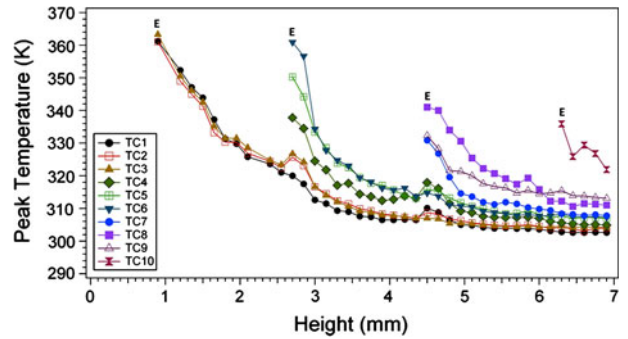


Fig. 9—History of peak temperatures attained at interfaces in the fabrication of the 46 layer build. The letter “E” indicated in the figure corresponds to embedding of thermocouples along an interface.

be observed from Figure 9, which shows the thermal history of all thermocouples during processing of the entire build. Every thermocouple registers a maximum temperature during its embedding and progressively lower temperatures as layers are added above. A saturation level is however observed to be reached because the progressively decreased heating at the bottom caused only a minimal temperature increase above ambient. As observed from Figures 8 and 9, TC1, TC2, and TC3 record the maximum number of data points, implying that the bottom-most layers are subject to the most transients. Strong cumulative effects with regard to the microstructure evolution noted previously^[9] (Section I) are therefore expected in these layers.

C. Heating of Stacked Thermocouples

The smoothed thermal profiles based on the three “vertically stacked” thermocouples TC8, TC5, and TC2 corresponding to processing of the 31st layer are shown in Figure 10. TC10 was not considered as part of these stacked thermocouples because it was observed to have moved considerably from its intended position even during its embedding (see next paragraph and Figure 12). From Figure 10, it may seem like TC5 and TC2 begin to heat up almost at the same instant. The profiles, however, are observed to peak one after the

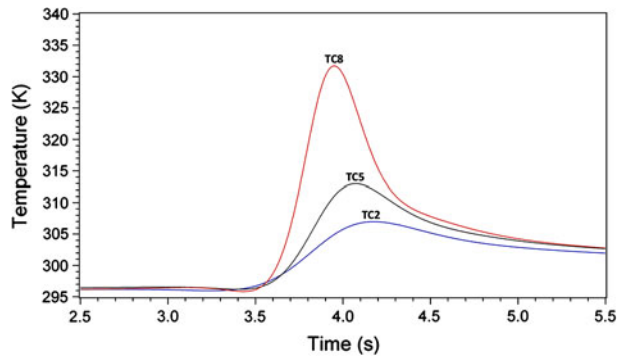


Fig. 10—Transients (smoothed) from a set of stacked thermocouples showing temperature rise occurring almost at the same instant.

other at discernible time intervals. It was thought to be interesting and important to ascertain whether the temperature increase in the stacked thermocouples TC8, TC5, and TC2 is consequent to heat being conducted down the build. As mentioned, work on low-power UAM had shown some peculiar behavior of stacked thermocouples.^[16] The time differentials Δt between the temperatures measured from TC8, TC5, and TC2, both with respect to 10 pct increase and peak values, are shown in Figures 11(a) and (b). The Δt values for the 10 pct increase in temperature (Figure 11(a)) are generally observed to be negative (except between TC5 and TC2 where most of the values are close to zero). The peak temperatures, in contrast, show Δt values that are consistently negative (Figure 11(b)). The negative values of Δt between top and bottom thermocouples would indeed be expected by the mechanism of heat conduction. The reason for near zero values (Figure 11(a)) between TC5 and TC2, however, is not readily understood. It is noted that the results (Figure 11) do not seem to follow any particular trend with the increasing number of layers or build height.

To understand such behavior (of the 10 pct increase in temperature) and the associated inconsistencies, it was decided to observe a longitudinal section of the build and locate the positions of the thermocouples on that section. An optical image of the section made along the center line of the build region containing the embedded thermocouples is shown in Figure 12. From this figure (Figure 12), it is immediately apparent that the thermocouples had moved from the intended positions (Figure 4). This is probably also the reason why TC4 could not be located on this longitudinal section. These could have resulted from the thin, lightweight thermocouple wires originally placed flush on the tape surface being swayed away by the vibrations as the sonotrode approached them. As was mentioned, such a tendency was actually observed during their embedding. Although this effect seems to have been significant on TC4 and TC10, it has also been strong with regard to TC7 and TC9. Given that TC8, TC5, and TC2 are not particularly well aligned vertically, it is possible that they start “experiencing” the heat at close time intervals (Figures 10 and 11(a)). A better understanding of this behavior was expected through modeling, which is presented in the next section.

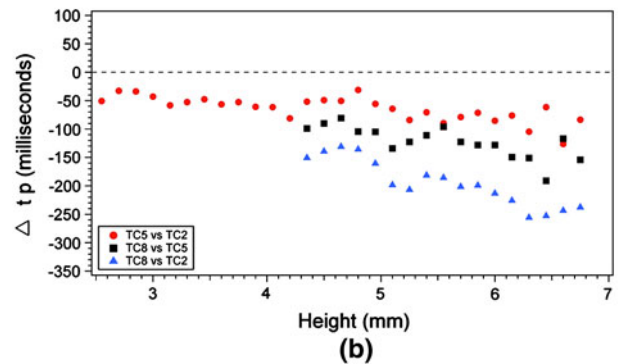
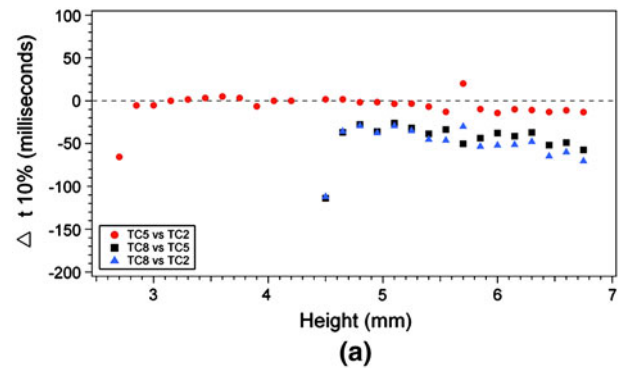


Fig. 11—Time differentials for stacked thermocouples corresponding to (a) 10 pct temperature increase and (b) peak temperatures. Negative values indicate a shorter time for the top thermocouple with respect to the bottom that would be expected from heat conduction.

D. Modeling of Temperature Increase/Simulation of Thermal Profiles

Figure 13 shows the simulated temperature contour distribution (at a given instant) resulting from a moving heat front for a build height of 4.5 mm and containing thermocouples at known positions (Figure 12). It is observed that TC2, although positioned below TC5, can fall into the same temperature contour, thus showing a similar temperature increase almost simultaneously. The peak temperatures attained by them, however, would be expected to occur in succession with a distinct time interval (Figures 10 and 11(b)).

The results of the simulated/predicted profiles are shown in Figure 14. The profiles are overlaid manually on the experimental transients to make the temperature increase instant in both cases coincident. It may be recalled (Section III) that simulations were run for a time interval of 3 seconds only (corresponding to distance of 101.6 mm); the primary objective was to capture just the transient stage. The peak temperature from the simulated profile for TC8 is observed to agree well with that measured experimentally (Figure 14(a)), as was intended. However, a close match has not been possible with respect to the heating and cooling rates, with the simulated profile being a little steeper and narrower than the experimental transient (Figure 14(a)). It was, however, interesting to note that the modeled profiles from bottom thermocouple locations (TC5 and TC2) resulting thereof exhibited nearly the same peak

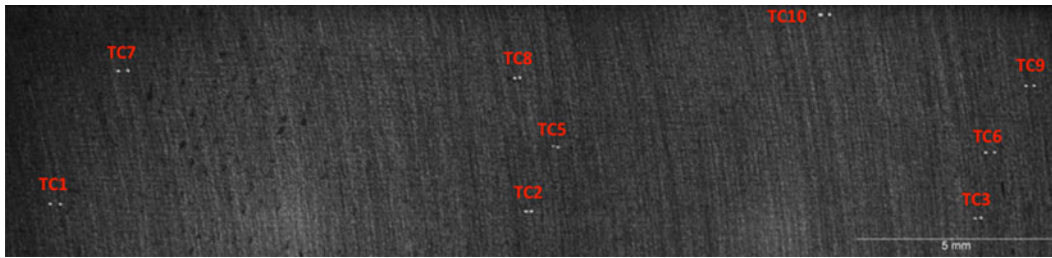


Fig. 12—Optical image of longitudinal section (along weld direction) close to center showing “actual” position of thermocouples. TC4 could not be located in this section.

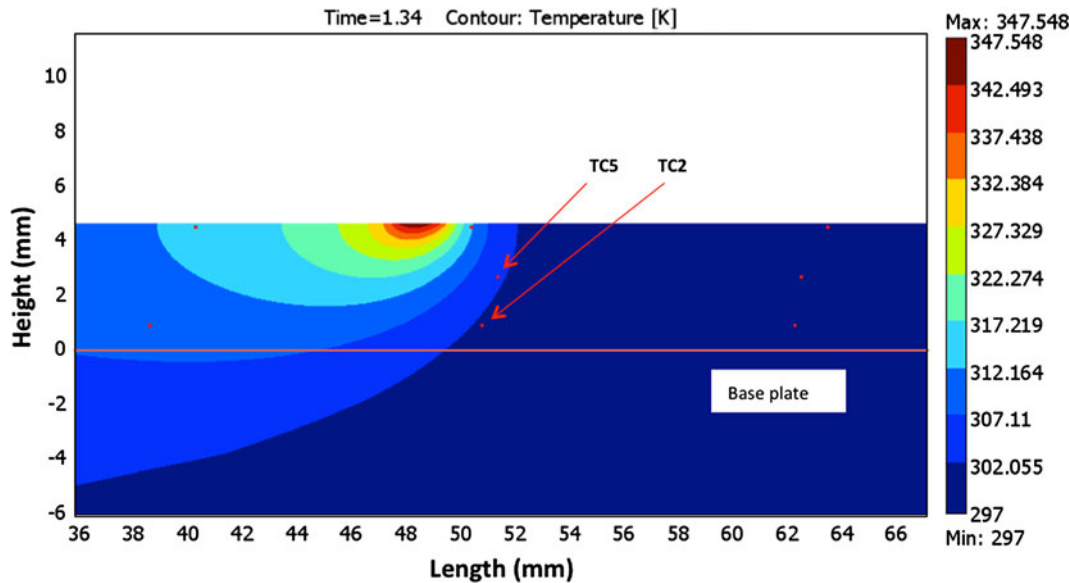


Fig. 13—Simulated temperature contours across the build height (of 4.5 mm) based on a 2-D heat conduction finite-element model. Both TC5 and TC2 can heat up to the same temperature almost at the same instant.

temperatures as the measured values (Figures 14(b) and (c)). This finding suggests that heating the bottom layers while processing a top layer is simply an effect of conduction. If any localized heating of the bottom layers occurred along with the top layer, as was hypothesized to occur in low-power UAM,^[16] it would have pushed the peak temperatures of TC5 and TC2 higher because of the combined effects of such local heating and conduction. However, such a phenomenon is not observed. The temperature increase across the build (as shown in Figure 8, for instance) can therefore be explained as an effect of heat being conducted away from the source (the top layer processed). The heating rates of the predicted profiles, however, differ from the experimental counterparts, although the maximum cooling rates are nearly similar (Figures 14(b) and (c)). Possible reasons for these are discussed subsequently.

Meanwhile, it was also thought pertinent to determine the time differentials from predictions with respect to the stacked thermocouples and compare them with experimental results (Figure 11). These are shown in Table II. The time differentials from predictions are observed to be of the order of milliseconds only, as was noted from experimentation (Figure 11). Although the magnitudes of the values are different, the trends, with regard to

which thermocouple heats up first, can be stated as being similar. The temperatures from TC8, TC5, and TC2 clearly peak one after the other here again (as observed in Figure 11(b)). This finding indicates that the build behaves almost like solid aluminum and also shows that the model is consistent within itself. A similar analysis was done for the other sets of stacked thermocouples as well (Table III). The trends with respect to the peak temperatures are consistent with the previous stacked thermocouples. However, small discrepancies are noted with regard to the 10 pct rise.

Despite good prediction of peak temperature values, a close match between the simulated and experimental profiles has not been possible. The fit, however, gets better with the bottom thermocouple locations. This could be related to the occurrence of rapid heating and cooling close to the heat source. Further down, in the bottom thermocouple locations, because the thermal gradients are low, the agreement might be better. The observed discrepancies between the simulated/predicted profiles and the experimental profiles could thus be attributed to the following reason.

The temperature transients measured are based on how the thermocouples are actually positioned/oriented within the build. They are expected to be values

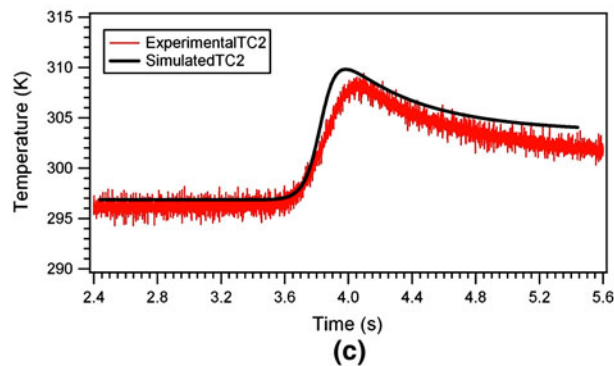
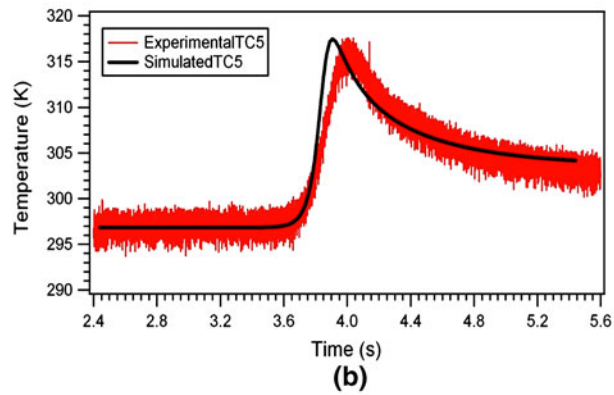
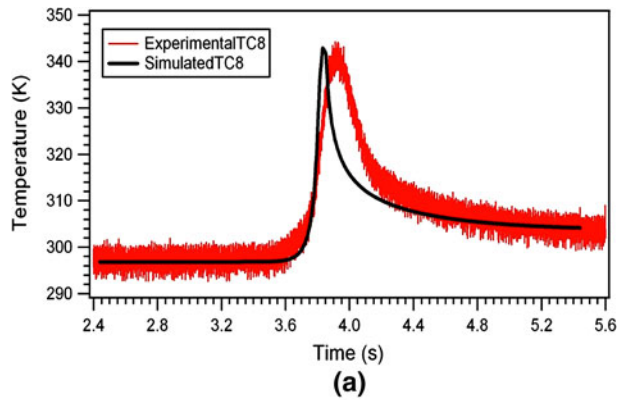


Fig. 14—Comparison of simulated/ predicted profiles to experimental transients for stacked thermocouples. (a) TC8, (b) TC5, and (c) TC2. A good agreement in peak temperatures is observed.

averaged over the surface area the thermocouples make contact with the surrounding material along their entire twisted length, in addition to being time averaged. Simulations and predictions, in contrast, pertain to “points” corresponding to the “coordinates” of the thermocouple wires on the given longitudinal section. These basic differences between measurements and simulations could reflect on a higher slope in the simulated profiles. Furthermore, for the sake of simplicity, a 2-D model that assumes the heat source to have a constant Q both along its length (over the width of the tape) and its thickness has been employed. In reality, Q from the “heat source” during VHP UAM processing, is expected to vary in both dimensions because of the presence of lateral vibrations, and the variation in normal force, which give rise to such

Table II. Comparison of Time Differentials Between Experimental and Simulated/Predicted Values for Stacked Thermocouples TC8, TC5, and TC2, for Heat Source at 4.5 mm Height

	Δt^* for 10 pct rise (ms)		Δt^* for Peak T (ms)	
	Measured	Predicted	Measured	Predicted
TC8 vs TC5	-114	-36	-90	-74
TC5 vs TC2	+2	-6	-49	-75
TC8 vs TC2	-112	-42	-139	-149

Table III. Comparison of Time Differentials Between Experimental and Simulated/ Predicted Values for Other Stacked Thermocouples (Corresponding to Heat Source at 4.5 mm Height)

	Δt^* for 10 pct Rise (ms)		Δt^* for Peak T (ms)	
	Measured	Predicted	Measured	Predicted
TC7 vs TC1	-114	17	-88	-93
TC9 vs TC6	-17	-17	-61	-18
TC6 vs TC3	-9	20	-90	-77
TC9 vs TC3	-26	3	-151	-95

heating. [The normal force exerted by the sonotrode on the tape (responsible for the contact stresses between tapes/layers) is expected to assume a bell-shaped profile^[24]—being maximum at the center of the contact region and decreasing towards the edges and along both the width and the length of the tape]. Discrepancies in profiles could have occurred because of these differences. The same argument holds for magnitude differences noted in the time differential values between the predicted and measured peak temperatures (Tables II and III), although the trends are observed to agree well.

Minor inconsistencies in the time differentials to the 10 pct temperature increase within the measured values (Figure 11(a), Tables II and III) could also have arisen because of the previously mentioned reasons. The possible change in the contact stress characteristics between welded layers may have played a role as well. Furthermore, it is quite obvious that such a small increase in temperature from ambient is expected to be sensitive to measurement procedures and analyses.

E. Implications of the Current Results

The results show that thermal transients are set up all across a multilayer build whenever a new layer is added to it. The bottom layers and interfaces, therefore, are subject to multiple thermal cycles with progressively decreasing peak temperatures. This could have a cumulative effect on microstructure evolution, both in the bulk of the tapes and the interfaces (as was observed in

our previous investigations on shorter builds)^[9] and ultimately on the bond quality itself layer after layer.

The results also indicate that the degree of bonding along the build could vary right at the time of processing a new layer. This depends on the height at which the layer is welded as was evidenced by a decrease in measured interfacial temperatures, and is probably the result of a loss in the ultrasonic energy transferred to the weld region. The hypothesis is that the ultrasonic energy applied to the foil translates itself into inducing dynamic plastic shearing of asperities between faying surfaces. Such shearing consequently leads to adiabatic heating, with at least 95 pct of the plastic work being converted into heat.^[25] This heat generation triggers a temperature increase causing bonding through interfacial DRX.^[11] The efficiency of transfer of ultrasonic energy to the weld region would be related to how effectively the vibrations are used into inducing plastic shearing. This depends essentially on the processing condition chosen—namely the vibration amplitude and normal force. With the normal force manifesting itself into a contact stress between the faying surfaces, this contact stress and its distribution could change with the addition of new layers to the build, even if the applied normal force were to be kept the same. (A detailed finite-element analysis of contact compressive stresses across layers could lead to a better understanding of this phenomenon.) This, consequently, is expected to influence the amount of energy being put into the weld for the chosen amplitude. However, with only a 5 pct decrease in homologous temperature, the energy loss is only marginal and is not expected to cause any significant influence on bond quality (and interfacial microstructures). Variations in temperature increase even along an interface could be attributed to changes in contact stresses locally. It is perhaps of relevance to mention from the work of past investigators^[26,27] that bonding has been observed to be influenced with build height. Based on their studies on low-power UAM, when the height of the build reached 0.7 to 1.2 times its width, a significant deterioration in bonding was observed. The phenomenon was attributed to a possible reduction in the stiffness of the “tall substrate”^[26] and the possible formation of destructively interfering standing waves that are harmonics of the fundamental frequency (20 kHz).^[27] However, it is noted that the height of the build in this current research is much lower (6.9 mm) for a tape width of 25.4 mm, and therefore such a phenomenon was not to be expected and not observed. [Optical microscopic examination of a transverse section of the build revealed minimal voids (estimated void fraction of only approximately 0.01 to 0.02) throughout the build including the top most layer with no indication of any gradient.]

To obtain an idea of the ultrasonic energy going into the weld during processing (and the possible energy loss), a simple estimate is worked out.

Based on the assumption that a minimum of 30 pct of the electrical power consumed by the process reaches the weld region as vibratory power,^[28] the vibratory power can be estimated to be at least $0.30 \times 1190 \text{ W} =$

357 W. The figure of 1190 W is the estimated average electrical power drawn for the processing parameters employed, which is based on the power measurement readings obtained from the machine during previous experiments.^[29]

For the given conditions of processing namely 26 μm , 5.6 kN, and 35.5 mm/s, the contact area the sonotrode makes with the tape is taken to be 2 mm \times 25.4 mm. The value 25.4 mm corresponds to the width of the tape, and 2 mm is the width of the imprint left by the sonotrode under the said normal force without any vibrations.^[10] The power per unit area going to the weld, therefore, is at least

$$\frac{\text{Power}}{\text{Area}} = \frac{357\text{W}}{2 \times 25.4 \text{ mm}^2} = 7 \frac{\text{W}}{\text{mm}^2} \quad [1]$$

The corresponding energy per unit area can be estimated as follows:

$$\begin{aligned} \frac{\text{Energy}}{\text{Area}} &= \left(\frac{\text{Power}}{\text{Area}} \right) \times \text{weld time} \\ &= \left(\frac{\text{Power}}{\text{Area}} \right) \times \left(\frac{\text{Contact width}}{\text{Travel speed}} \right) \end{aligned} \quad [2]$$

Therefore, the minimum amount of energy per unit area would be

$$\frac{\text{Energy}}{\text{Area}} = \left(7 \frac{\text{W}}{\text{mm}^2} \right) \times \left(\frac{2 \text{ mm}}{35.5 \frac{\text{mm}}{\text{s}}} \right) = 0.4 \frac{\text{joules}}{\text{mm}^2} \quad [2a]$$

Assuming that 100 pct of the energy is used up for plastic shearing of asperities (without any loss in energy) and given that 95 pct of plastic work is converted to heat,^[26] the heat flux density at the weld region is estimated to be

$$Q = 0.95 \times 7 = 6.6 \frac{\text{W}}{\text{mm}^2} \quad [3]$$

It is observed that this value is 23 pct higher than the Q value chosen for modeling (5.1 W/mm²), which could imply that the energy going to the weld is lower. So rather than 100 pct of energy being used for plastic shearing, only 77 pct is probably used. The loss in energy conversion could even get higher with build heights as was observed experimentally. This is under the assumption that only 30 pct of the electrical power is converted to vibratory power.

The results from modeling reveal that the temperature rise in bottom interfaces could simply be an effect of heat conducted away from the top. Heat across a layer is extracted within the order of only milliseconds attributable to the high thermal conductivity of aluminum. Modeling based on the temperature contour distribution arising out of such a moving heat front has also demonstrated that the bottom layers could experience heating even when the heat source is not right on top of it along the vertical plane. The heating pattern in VHP UAM, therefore, can be represented by a schematic as

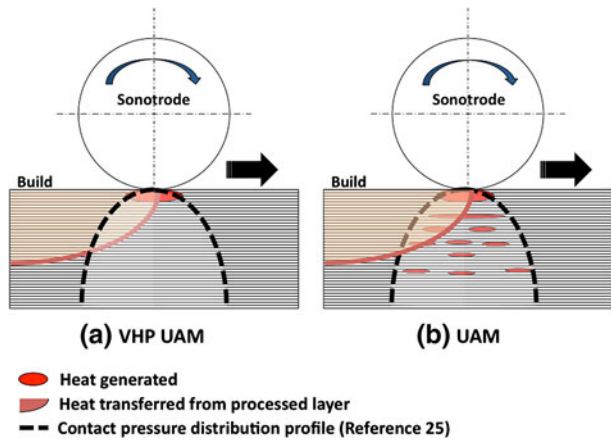


Fig. 15—Schematic showing the heat generated at the processed layer during VHP UAM and being conducted away through the build (a). Previous work by Schick *et al.*^[16] suggests localized heating at multiple interfaces in low-power UAM depicted by (b).

shown in Figure 15(a). The possible nature of the contact stress distribution profile beneath the sonotrode is also indicated (Figure 15(a)). This is in contrast to what is suggested (Figure 15(b)) from the work of Schick *et al.*^[16] because of the poor bond quality in low-power UAM. The thermal behavior of the multilayer build produced by VHP UAM can, therefore, be considered almost equivalent to that of an aluminum block indicating superior bonding.

V. CONCLUSIONS

Thermal transients generated during processing of a 3003 Al-H18 multilayer build by VHP UAM were investigated. Processing was done for the parameters 26 μm amplitude, 5.6 kN normal force, and 35.5 mm/s travel speed without any external heating using a sonotrode surface texture of $R_a = 7 \mu\text{m}$. Based on this research, the following conclusions are drawn:

1. Transients are set up along and across a multilayer build during processing of every layer.
2. Multiple thermal cycles are experienced by every layer/interface below. The temperatures reached and the associated heating/cooling rates in these layers diminish with every cycle. This explains the cumulative effects on microstructure evolution observed earlier and could also lead to a gradient in bonding.
3. The temperatures generated during the process can also depend on the layer being processed (build height). A decrease in temperatures (2 pct, in terms of homologous temperatures) with increasing build heights is observed because of a possible decrease in ultrasonic energy going to the weld. This could add to the cumulative effects influencing bonding in those layers.
4. Modeling based on classic conductive heat transfer has shown that transients in the bottom layers can be rationalized in terms of heat conduction, expected in

3003 Al, from the weld region of the layer processed to other parts of the build.

5. VHP UAM using 3003 Al tapes can thus produce parts with thermal properties close to that of a solid 3003 aluminum block.

Future work could involve mechanical testing of multilayer builds and evaluating possible gradients in bond strength. The microstructure evolution across the build could also be investigated in detail. Modeling of the heating phenomena using a vibrating (and traveling) heat source under contact pressure may lead to a better understanding of the thermal behavior in builds made by VHP UAM. It may also be imperative to model the effect of voids on heat transfer characteristics. Tracking the temperatures of the surface layer could be considered a possible nondestructive method of evaluating bonding quality *in situ*.

ACKNOWLEDGMENTS

The authors sincerely thank Ohio Department of Development for funding this research through the Third Frontier Wright Projects program. The support and encouragement received from Dr. Karl Graff of Edison Welding Institute is acknowledged gratefully. Thanks are also due to Matt Short, Mark Norfolk, Paul Boulware, and other colleagues from Edison Welding Institute, and to Dr. Marcelo Dapino of Mechanical Engineering Department, Ohio State University for their assistance in carrying out this research.

REFERENCES

1. D.R. White: *Adv. Mater. Process.*, 2003, vol. 161, pp. 64–65.
2. C.Y. Kong, R.C. Soar, and P.M. Dickens: *J. Mater. Process. Tech.*, 2004, vol. 146, pp. 181–87.
3. K. Graff: private communication, April 30, 2009.
4. S.S. Babu, O. Barabash, and K. Graff: Edison Welding Institute, Columbus, OH, unpublished research, 2010.
5. D.E. Schick, R.M. Hahnen, R. Dehoff, P. Collins, S.S. Babu, M.J. Dapino, and J.C. Lippold: *Weld. J.*, 2010, vol. 89, pp. 105–15.
6. M.R. Sriraman, S.S. Babu, and M. Short: *Scripta Mater.*, 2010, vol. 62, pp. 560–63.
7. M.R. Sriraman, H. Fujii, M. Gonser, S.S. Babu, and M. Short: *Proc. 21st Int. Solid Freeform Fabrication Symp.*, Austin, TX, 2010, David L. Bourell, ed., 2010, pp. 372–82.
8. K. Sojiphan, M.R. Sriraman, and S.S. Babu: *Proc. 21st Int. Solid Freeform Fabrication Symp.*, Austin, TX, 2010, ed., David L. Bourell, 2010, pp. 362–71.
9. H. Fujii, M.R. Sriraman, and S.S. Babu: *Metall. Mater. Trans. A*, 2011, in press.
10. M.R. Sriraman: The Ohio State University, Columbus, OH, unpublished research, 2011.
11. M.R. Sriraman, M. Gonser, H. Fujii, S.S. Babu, and M. Bloss: *J. Mater. Process. Tech.*, 2011, vol. 211, pp. 1650–57.
12. Y. Yang, G.D. Janaki Ram, and B.E. Stucker: *J. Mater. Process. Tech.*, 2009, vol. 209, pp. 4915–24.
13. I.E. Gunduz, T. Ando, E. Shattuck, P.Y. Wong, and C.C. Doumanidis: *Scripta Mater.*, 2005, vol. 52, pp. 939–43.
14. M.A. Meyers, J.C. LaSalvia, V.F. Nestorenko, Y.J. Chen, and B.K. Kad: *Proc. Third Int. Conf. on Recrystallization and Related Phenomena (ReX '96)*, Terry R. McNelley, ed., Monterey Institute for Advanced Studies, Salinas, CA, 1997, pp. 279–86.
15. U. Andrade, M.A. Meyers, K.S. Vecchio, and A.H. Chokshi: *Acta Metall. Mater.*, 1994, vol. 42, pp. 3183–95.

16. D.E. Schick, S.S. Babu, D. Foster, M. Short, M.J. Dapino, and J.C. Lippold: *Rapid Prototyp. J.*, 2011, vol. 17 (5), pp. 369–79.
17. E.L. Rooy: *ASM Handbook Online*, 1990, vol. 2, pp. 62–122, <http://products.asminternational.org/hbk/index.jsp>.
18. C.Y. Kong, R.C. Soar, and P.M. Dickens: *Compos. Struct.*, 2004, vol. 66, pp. 421–27.
19. M.R. Sriraman, S.S. Babu, M. Short, and K. Graff: *Proc. Second Symposium on Ultrasonic Additive Manufacturing*, Edison Welding Institute, Columbus, OH, 2009, pp. E69–73.
20. P. Boulware: private communication, May 5, 2010.
21. A.M. Ramirez, F.J. Espinoza Beltran, J.M. Yanez-Limon, Y.V. Vorobiev, J. Gonzalez-Hernandez, and J.M. Hallen: *J. Mater. Res.*, 1999, vol. 14 (10), pp. 3901–06.
22. A.N. Abramenko, A.S. Kalinichenko, Y. Burtser, V.A. Kalinichenko, S.A. Tanaeva, and I.P. Vasilenko: *J. Eng. Phys. Thermophys.*, 1999, vol. 72 (3), pp. 369–73.
23. G.E. Totten and D.S. MacKenzie: *Handbook of Aluminum Volume 2: Alloy Production and Material Manufacturing*, Marcel Dekker Inc., New York, NY, 2003, pp. 716–18.
24. E.J. Hearn: *Mechanics of Materials*, 3rd ed., Butterworth-Heinemann, Burlington, MA, 1997, vol. 2, pp. 381–411.
25. G.E. Dieter: *Mechanical Metallurgy*, 3rd ed., McGraw-Hill Book Co., New York, NY, 1986, pp. 503–63.
26. C.J. Robinson, C. Zhang, J.G.D. Ram, E.J. Siggard, B. Stucker, and L. Li: *Proc. 17th Int. Solid Freeform Fabrication Symposium*, Austin, TX, 2006, David L. Bourell, ed., 2006.
27. C. Zhang and L. Li: *Proc. 17th Int. Solid Freeform Fabrication Symposium*, David L. Bourell, ed., Austin, TX, 2006.
28. A.L. Phillips: *Ultrasonic Welding*, American Welding Society, NY, 1960, pp. 2–36.
29. M.R. Sriraman: The Ohio State University, Columbus, OH, unpublished research, 2009.